JOURNAL OF OPTOELECTRONICS AND ADVANCED MATERIALS Vol. 10, No. 3, March 2008, p. 520 - 527

Doped cadmium sulfide particles in polymer matrix: X-ray diffraction, optical reflectivity and photoconductivity study

J. FRANC*, S. NEŠPŮREK[a], M. V. MAKAROVA, P. KRTIL
J. Heyrovský Institute of Physical Chemistry of ASCR, v.v.i., Dolejškova 3, 18223 Praha 8, Czech Republic
[a]Institute of Macromolecular Chemistry of ASCR, v.v.i., Heyrovský Sq. 2, 162 06 Praha 6, Czech Republic

Photosensitive powders of cadmium sulphide doped with donors (Cl^-, from 0 to 41 mg/g CdS) and acceptors (Cu^{2+} and Ag^+, from 0 to 9 mg/g CdS) were characterized by granulometry, scanning electron microscopy, X-ray diffraction and optical reflectivity spectra. Incorporation of chloride ions caused the increase of band gap energy from 2.27 to 2.38 eV. Polystyrene, poly(methyl methacrylate), poly(*N*-vinylcarbazole), poly(bisphenol A carbonate) and epoxy resin were used as binders in pastes containing powders. Layers prepared from the pastes were characterized by reflectivity spectra and photonductivity. The layers composed of powders with low doping levels and binders containing bisphenol A group in the chain exhibited the highest photoconductivity.

(Received February 4, 2008; accepted

Keywords: Cadmium sulfide, Doping, Polymer binder, Photoconductivity, Optical reflectivity

1. Introduction

Cadmium sulphide (CdS) is used for a long time as a photosensitive material. Undoped crystal exhibits at 300 K a band gap 2.42 eV [1], which corresponds to absorption edge at 515 nm. Photoelectric sensitivity in the visible region considerably increases by the introduction of donors and acceptors. CdS is the compound of the type $A^{II}B^{VI}$. From this fact follows that metals of the group III (Al, Ga, In) and elements of the group VII (halogens) act as donors. On the other hand the acceptors form elements of the group V and metals of the group Ib, (Cu, Ag, Au). Silver and copper shift absorption onset to 2.0 and 1.7 eV, respectively. However, not only impurities from mentioned groups, but also point crystal imperfections and oxygen can form new electronic states. [2,3]. The halogens act simultaneously as fluxing agents [4].

Thick film technologies cut the production cost of electronic devices. An endeavour to use these techniques for the fabrication of solar cells and photosensors is then fully understandable [5,6]. The idea of the preparation of photoconductive layers from polymer dispersions is not new; the application of CdS phosphors with plastic binders was patented in 1943 [7]. Next authors studied dependence of photoconductivity on CdS powder treatment provided that binder - usually polystyrene (PS) - has no specific effect on grain properties. The photoconductivity increase in the presence of binder was ascribed to the better layer filling [8-10]. Current-voltage chacteristics of such layers exhibited parts with different slopes. This behaviour was explained by the changes of photoconductivity mechanisms. The light sensitivity of films comparable with the devices based on single-crystalline material was achieved at electric field strengths of about 10^4 V/cm. [11].

Later works were focused on interactions between CdS and organic components: polymers stabilizing colloid solutions [12], hole transporting poly(*N*-vinylcarbazole) (PVCA) [13], π-conjugated polymers [14,15], polyaromatic hydrocarbons and phthalocyanines [16], polyaniline [17-19] or amino groups with complexation ability [20,21].

Polymers for the preparation of the photoconductive pastes must fulfil several requirements. In particular, they must have relatively high molecular mass, which ensures the required viscosity, must be transparent in the region of the application, so that they could not absorb light necessary for charge photogeneration in photoconductive particles, and must contain some groups (in the main chain or pendant groups) which enable the charge transport at relatively low intergrain energetic barriers. With respect to the fact that polaron formation cannot be excluded, the polarizability of the system must be minimized.

We selected the following polymers: Polystyrene (PS) as representative of originally used matter, poly(methyl metacrylate) (PMMA) as the type of polymer without aromatic groups in the molecule, PVCA and poly(bisphenol A carbonate) (PC) as new types of polymers. Promising binder forms also epoxy resin based on diglycidyl ether of bisphenol A cured with diethylenetriamine, partly through aromatic group in the chain, partly trough amine groups, which are effective complexing agents with the CdS surface [20,21].

The aim of this work it was wide ranged screening of dopant doses in CdS particles to maximize the photoconductivity of layers with epoxide binder. Particles were also characterized by granulometry, scanning electron microscopy (SEM), reflectivity spectra and X-ray diffraction (XRD). Selected polymers were compared by the photoconductivity of thick layers using powder with the highest photoconductivity in epoxide binder.

2. Experimental

2.1. Powder activation and characterization

The starting material, CdS powder (pure, LVL Bad Liebenstein, Germany), was mixed with deionised water in a porcelain dish to form a mash. Then the solutions of dopants were consecutively introduced with stirring. The solutions of $AgNO_3$ and $CuCl_2$ as the acceptor sources and that of $MnCl_2$ as donor source were used. Data are summarised in Table 1. Silver and copper cations form chemical bonds on the grain surfaces. They replace Cd in cadmium sulphide because the solubility products of these metal sulfides are lower than that of cadmium sulphide. On the other hand $MnCl_2$ only dries up as salt on the grain surface during drying the mixture at 120 °C. The dry mixture was disintegrated to powder in porcelain mortar and sifted through a mill silk with mesh size 150 μm. A part of powder E was decanted in water after drying to wash chloride anions from a particle surface. The washed powder E represents the activation with Cu^{2+} and without a presence of Cl^-. The powders were placed in glass crucibles with a cover. Each crucible was put in a steel container and heated in air in muffle furnace to 530 °C for 1 hour. Before the final study different annealing regimes were tested; temperature and time ranged from 530 to 630 °C and from 30 to 80 minutes, respectively. The chosen annealing regime yielded the powders with the highest sensitivity to illumination.

Table 1. Dopant doses in CdS powders and powder content in the layers with epoxy binders.

Sample	Concentration of dopants [mg/g CdS]				Powder in layer
	Ag^+	Cu^{2+}	Mn^{2+}	Cl^-	[wt %]
A	0.00	0.00	0.00	0.00	68.6
B	0.08	0.40	0.00	0.47	75.2
C	0.15	0.75	0.00	0.87	68.9
D	0.24	1.20	0.00	1.40	62.8
E	0.00	1.60	0.00	1.86	62.8
F	0.40	2.00	0.00	2.33	62.6
G	0.60	3.00	0.00	3.50	63.1
H	0.80	4.00	0.00	4.66	63.0
I	0.00	0.00	1.36	1.75	68.3
J	0.08	0.40	1.36	2.22	68.2
K	0.15	0.75	1.36	2.62	68.4
L	0.26	1.20	1.36	3.15	68.4
M	0.00	0.00	2.52	3.25	67.9
N	0.08	0.40	2.52	3.72	68.1
O	0.15	0.75	2.52	4.12	67.8
P	0.24	1.20	2.52	4.65	69.7
Q	0.00	0.00	4.00	5.16	68.0
R	0.08	0.40	4.00	5.63	68.4
S	0.15	0.75	4.00	6.03	68.0
T	0.24	1.20	4.00	6.56	70.5
U	0.45	2.25	7.50	12.30	74.0
V	1.50	7.49	25.00	41.04	77.0

Granulometric analyses of prepared powders were carried out by particle size analyzer Cilas 1064 (France). SEM images were taken using Hitachi S-4800. The crystalline structures were checked by powder X-ray diffraction (XRD) with Bruker D8 Advance powder X-ray diffractometer equipped with Vantec-1 detector using Cu K_α radiation. Angle 2θ varied from 10 to 90 degrees. Chemical analysis of powders was carried out with x-ray energy dispersive spectrometry (EDS) using Noran System Six (Thermo Electron Corp., USA) connected with SEM. Spectral reflectivities of powders were measured in the range 200 – 2500 nm on 10 mm thick layers. UV-Vis-NIR spectrometer Lambda 19 Perkin Elmer (USA) with diffusion reflectance attachment with $BaSO_4$ integrating sphere was used. Experimental data were treated by Kubelka-Munk formula [22] which describes the optical absorption in the term of reflection:

$$\frac{K}{S} = \frac{(R_\infty - 1)^2}{2R_\infty} \tag{1}$$

where R_∞ is the reflectance at infinite thickness, K and S is absorption and scattering coefficient, respectively. Revised Kubelka-Munk theory [23] relates K and S to the fundamental optical parameters of solid and gives for diffuse light

$$K = 2\alpha \tag{2}$$

where α is the absorption coefficient. Scattering coefficient was considered to be the same for all samples. Optical band gap energy E_g was determined using standard expression for direct transitions between two parabolic bands

$$(\alpha E)^2 = \mathrm{A}(E - E_g) \tag{3}$$

where E is the photon energy and A is the constant for the given transition.

2.2. Organic binders

Epoxide resin type CHS epoxy 517 (Spolchemie Comp., Czech Rep.) was used in the most experiments. It was a low-molecular-weight resin (M_w = 365 g/mol) modified with a reactive dibutyl maleate, characterised by epoxide index 4.0 – 4.3 mol/1000g and maximum viscosity 1.2 Pas (23 °C).

The other polymers selected for the tests were dissolved in suitable solvents (Fluka). In the case of PS (Krasten 144, Kaučuk, Czech Rep.), 0.4 g of the polymer was dissolved in 1.6 ml of butyl acetate). After the shaking for several hours, a clear viscous solution was obtained, which need not be centrifuged. In the case of PVCA (BASF, Germany), 0.4 g of the polymer was dissolved in 1.6 ml of a mixture of cyclohexanone and toluene (1:1).

Chloroform was used for the dissolution of PC and PMMA (both Aldrich, USA), again 0.4 g in 1.6 ml.

The molar masses (M_w) of the polymers were determined using gel pressure chromatography (Laboratory Instruments, Czech Rep.). M_w and polydispersity M_w/M_n (SEC averages relative to polystyrene standards) are given in Table 2. The structural formulae of binders are shown in Fig. 1.

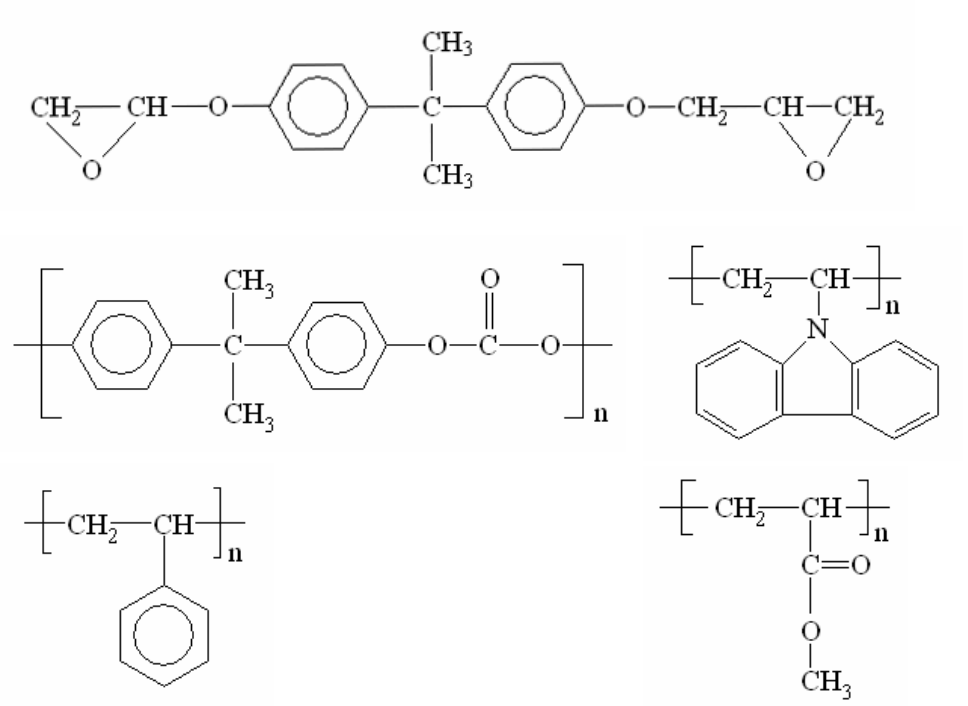

Fig. 1. The structural formulae of binders: a) CHS epoxy 517, b) poly(Bisphenol A carbonate) (PC), c) poly(N-vinylcarbazole) (PVCA), d) polystyrene (PS), e) poly(methyl methacrylate) (PMMA).

Table 2. Molar masses M_w and polydispersity M_w/M_n of selected polymers.

Polymer	M_w (10^3g/mol)	M_w/M_n
PMMA	368	2.50
PS	994	1.76
PC	24	2.11
PVCA	613	3.90

2.3. Coating of layers; reflectivity and photoconductivity measurement

The binder and activated powder were weighed into a porcelain dish and the mixture was homogenized with a masher. The contents of powder in the layers used in screening of dopant doses are given in Table 1. A percolation threshold was exceeded in all cases. Pastes were applied on alumina substrates by stenciling. The layer sample was ring-shaped with diameter of 20 mm. The metal foil stencil was 0.1 mm thick. The layers based on dissolved polymers were dried up at 50 °C for 1 h. Epoxy resin was cured 1 h at 180 °C.

Spectral reflectivity (Lambda 19 Perkin Elmer) and electrical conductivity were measured on the layers. For conductivity measurements the samples were equipped with indium electrodes evaporated on the top of the layer. The electrode distance was 0.7 mm and the meander length was 233 mm. The following procedure was applied: after the application of voltage (100 V) and sample stabilization, the dark resistance and the change in resistance due to the sample illumination (1000 lx) were measured. A tungsten filament light bulb (60 W, 2600 K) and ohmmeter IM5E (Radiometer Copenhagen, Denmark) were used.

3. Results and discussion

3.1. Granulometric analyses, habitus and morphology of grains

Particle size of starting CdS powder ranged from 0.6 to 56 μm; 97% of particles is distributed between 14 and 56 μm with maximum frequency at 25 μm. No shift to larger grain sizes was observed after the activation of the

powders except of powder V (see Table 1), where the concentration of chlorides was high enough to cause a particle sintering.

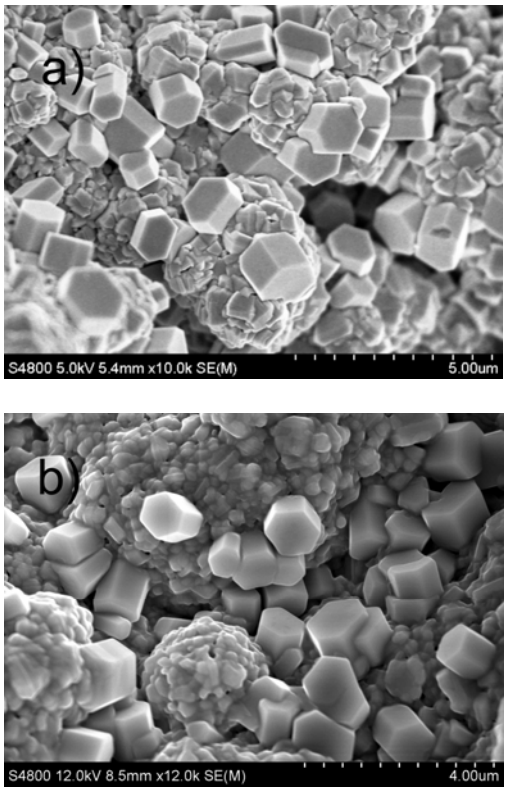

Fig. 2. SEM images of starting CdS powder (a) and sample A (b).

The particles of starting CdS powder are shown in Fig. 2a. It is clear that grains presented by granulometry as the particles with the diameter of tens of micrometers are in fact agglomerates of submicron particles and prismatic crystals with dimensions about 1 micron. The cross section of prismatic crystals is mostly irregular hexagon; the shape of smaller crystallites is less resolved. The characteristic shape of particles with hexagonal cross section may be taken as an indicator of hexagonal syngony of prismatic crystal, the structure of which could correspond to wurtzite structural type. The shape of the submicron particles gives no indication of its crystalline structure. The SEM image of sample A (Fig. 2b) illustrates the concretion of submicron particles at activation temperature without admixtures. The heating activation in presence of admixtures seems to result in growth of the prismatic crystal with hexagonal cross section. This growth proceeds at the account of submicron crystals originally present in starting CdS. The growth development at the increasing content of $AgNO_3$ and $CuCl_2$ (samples B, D) is shown in Fig. 3. The compact grains with stepwise-structured surface are formed during activation. Increasing content of $MnCl_2$ (samples I, M, Q) and also combinations of all admixtures act in similar way.

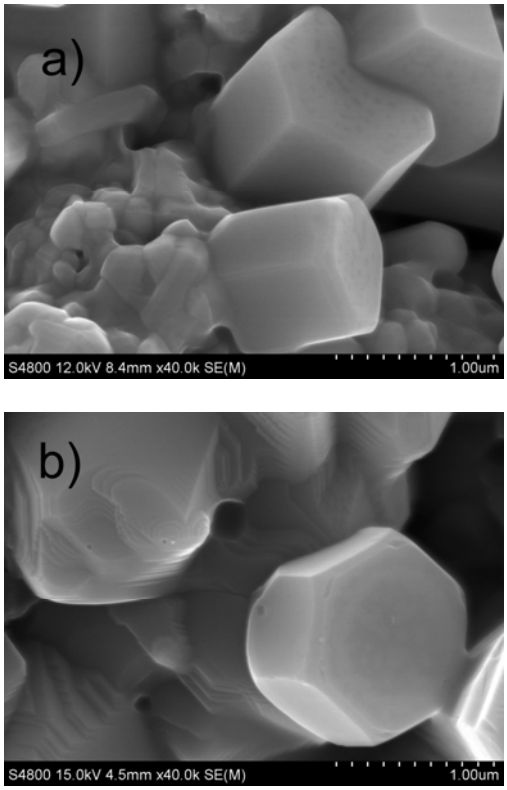

Fig. 3. SEM images of powders B (a) and D (b).

3.2. Chemical and structural characterization

We found the composition of starting and modified powders expressible as CdS_x, where x = 0.969 with standard deviation σ = 0.013. Such a slight non-stoichiometry indicates the presence of sulphur vacancies, which is in agreement with usual n-type of CdS conductivity.

Characteristic XRD patterns of starting and modified CdS samples are summarized in Fig. 4. The analysis of pattern of starting CdS shows that the powder is a mixture of hexagonal (40 %) and cubic (60 %) phases. The heat activation shifts the ratio between phases in favour of hexagonal polymorph (to 70 %) at sample A. All other samples activated with dopants transform completely to hexagonal phase (see Fig. 4). This result agrees with conclusions given in Ref. [24] but in our case the complete transformation took place at substantially lower $CuCl_2$ concentrations (in comparison with 1 % $CuCl_2$ presented in Ref. [24]). The importance of chloride anions for the phase transformation was further checked on washed powder E. Activation without Cl^- yields the material containing 12.5 % of cubic phase.

A content of other phases except mentioned CdS ones (such as $CdSO_4$ or MnS) did not exceed 1 %. Lattice constants of the phases found in sample A were a = 4.137 Å and c = 6.717 Å for hexagonal phase (greenockite) and a = 5.831 Å for cubic phase (hawleyite). These values are in good agreement with those reported in Ref. [25] and [26], respectively. The incorporation of the dopant does

not lead to a significant change (on the first two decimal places) of the lattice constants of the hexagonal phase.

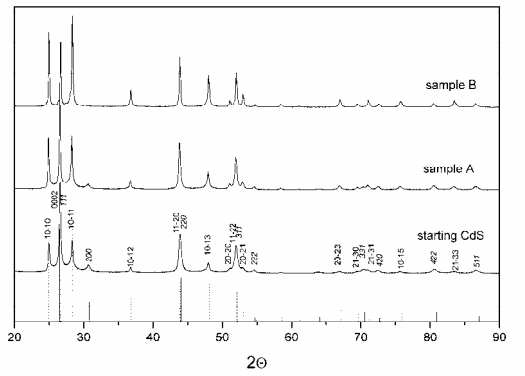

Fig. 4. XRD spectra of starting CdS and samples A and B. The peaks indexed in italic appertain to the cubic phase (solid lines), the other to the hexagonal phase (dotted lines).

3.3. Dopant diffusion

The penetration of dopants in the CdS matrix may be approximated by Arrhenius type of behaviour for diffusion coefficient:

$$D = D_0 \exp(-Q/RT)$$

where D_0 stands for frequency factor and Q for activation energy. The actual diffusion coefficient values calculated for doping cations using previously reported data [4,27,28] allow to estimate effective diffusion depths:

$$x = \sqrt{2Dt} \tag{5}$$

where t is the time [29]. Keeping in mind the actual activation conditions and assuming linear semi-infinite diffusion we arrive to estimated diffusion depth of Cu and Ag of approximately 130 μm. This indicates that one can expect more or less homogeneous distribution of Cu and Ag within the grains. The same procedure for Mn and Cl gives less reliable estimate. The available literature data on these systems [4,30] are related to significantly higher temperatures (1150 °C and 800 °C) and even at such elevated temperatures they lay behind those of Cu and Ag at 530 °C by an order of magnitude. That restricts the expected diffusion depth to cca 1 μm. Comparing the effective diffusion depth of dopants with particle size of individual crystal one sees that these values are really comparable so we can also expect more or less homogeneous distribution of Mn and Cl in the structure.

3.4. Spectral reflectivity of powders

Activation process changed the colour of cadmium sulphide powder depending on kind and concentration of dopants. Exact characterization was done by the measurement of reflectivity spectra. Spectra of selected powders are shown in Fig. 5. Undoped sample A showed a well-developed edge on the spectral curve enabling the estimation of band gap energy as 2.27 eV. The activation only with $MnCl_2$ caused only weak long-wave tail on the spectral curve. The band gap could be estimated as 2.38 eV. The comparison with the published value 2.42 eV [1] suggests that the observed increase in the band gap energy is caused by the disappearance of some energetic levels from a band gap after the incorporation of chloride anions to CdS. If $CuCl_2$ and $AgNO_3$ were used in the activation, a significant absorption at longer wavelengths appeared. Therefore, the estimation of CdS band gap was impossible by the methods described above.

Reflectivity of samples reached its minimum at wavelengths around about 400 nm. All samples showed similar values between 9.3 and 14.7%. The highest values (13.9-14.7%) belonged to the samples activated with $MnCl_2$ only (samples I, M, Q), the lowest values (9.3-10.4) belonged to the samples doped at low (samples A, B) and high (samples U, V) level. The reflectivity of the other samples was observed in range 10.8 -12%.

The maximum reflectivities of powders under study were found at wavelengths over 800 nm; the values occurred in wide range 31.0 - 97.9%. The highest value showed the undoped sample A and the reflectivity decreased with the growing content of acceptors (Cu, Ag). Keeping the content of acceptors the same, the reflectivity decreased with growing chloride amount.

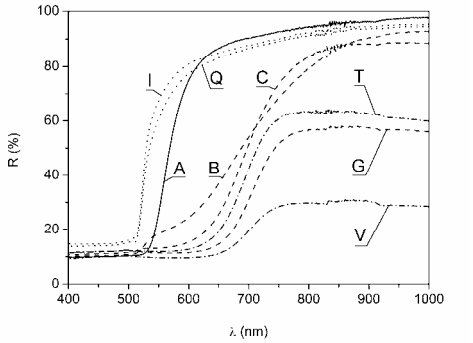

Fig. 5. Selected reflectivity spectra of powders. The style of lines corresponds to the doping substances: solid – undoped sample, dot – $MnCl_2$, dash – $AgNO_3$ + $CuCl_2$, dash - dot – all. Lettering of samples corresponds to Table 1.

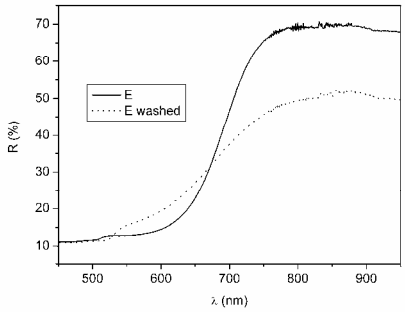

Fig. 6. Reflectivity spectra of powder E and of that washed before annealing. Experiment illustrates the effect of chloride anions on the steepness of characteristic at an absorption edge.

Comparing characteristics of washed powder E and powder E we found that activation without Cl^- leads to absorption spectrum with less steep increase of the absorbance near the absorption edge (see Fig. 6). This may be with high probability correlated with higher concentration of structural defects in the powder. Also the reflectivity at 900 nm was lover than at unwashed powder. This fact indicates that some amount of chloride influences both the band gap energy and reflectivity at 900 nm.

3.5. Spectral reflectivity of layers with polymer binder

The reflectivity spectra enabled the determination of radiance portion that was absorbed in the layers. We supposed that the non-reflected part was fully absorbed in CdS layer. The radiation penetrating into the substrate was neglected. Fig. 7 shows the reflection spectra of alumina substrate and that covered with the layer of epoxide binder. The reflectivity decreased in the region of wavelengths shorter than 500 nm; thus the big part of radiation can penetrate into the substrate. However, in this region CdS exhibits high absorption. Besides the portion of such light in the bulb spectrum is small. In the region between 500 - 1300 nm the substrate reflectivity reached the highest value; thus the radiation penetrating into the substrate might also be neglected. Radiation with wavelengths longer than 1300 nm is partially absorbed in epoxide binder, these quanta, however, do not contribute significantly to the charge carrier generation in CdS.

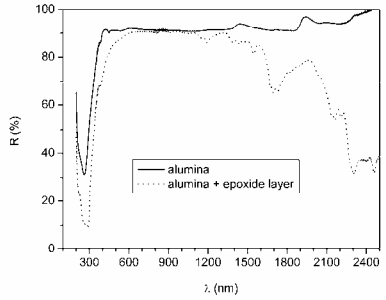

Fig. 7. Reflectivity spectra of bare alumina and alumina covered with epoxide layer.

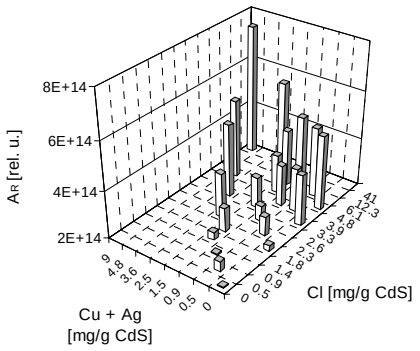

Fig. 8. Relative absorbed doses A_R in the range 200 – 1300 nm (Eq. 6) in dependence of dopant concentration.

Relative absorbed doses A_R in the range 200 – 1300 nm can be calculated using the equation:

$$A_R = \int_{200}^{1300} (1 - R_\lambda) H_\lambda \, d\lambda \,, \qquad (6)$$

where R_λ is spectral reflectivity of layers with epoxy binder and H_λ is the spectral intensity of incident light (approximated by Plank's law of black body radiation, corrected for the tungsten emissivity [31]). Value of A_R increased with growing amount of dopants; its maximum value was 3.6 times higher than the minimum one (see Fig. 8).

Reflectivity of 0.1 mm thick layer consisting of the powder and epoxy binder was lower in the UV and visible range than that of 10 mm thick layer of the corresponding powder. It may be ascribed to the value of refractive index of epoxide binder. It means the binder acts as antireflection coating. Very striking decrease of reflectivity was observed when powder was activated only with $MnCl_2$ (see Fig. 9). Such a decrease was not observed neither for the other selected polymers nor for epoxy binder cured at room temperature. One can speculate about chemical reaction between free chloride anions and the epoxide binder.

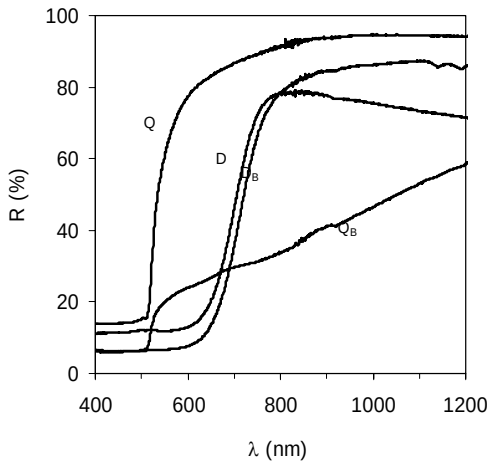

Fig. 9. Differences of spectral reflectivities of powders with (index B) and without epoxy resin binder. Powder activated with $MnCl_2$ only (Q) and powde r without $MnCl_2$ activation (D).

3.5. Photoconductivity

The photoconductivity of all powders was studied using the layers based on epoxide binder. Relative absorbed doses of the radiance A_R varied in the range being less than one order of magnitude. On the other hand photocurrents I_L decreased by three orders of magnitude with growing dopant concentrations. Maximum photocurrent achieved sample B, i.e. the sample with the lowest dopant level. Powders activated with the highest dopant concentrations (samples U and V) were probably degenerated (no photoconductivity was observed).

Comparison of I_L with corresponding A_R value indicated that with growing dopant concentrations decreases the efficiency of absorbed light conversion.

Considering a functional application we focused on the ratio of the photocurrent I_L and dark current I_D. The dependence of I_L/I_D ratios on dopant concentrations are shown in Fig. 10. Maximum value 1.3×10^6 we found for sample E. Sample E was also used to compare the influence of the selected polymer binders. Results are summarised in Table 3. The highest I_L/I_D ratio was achieved in PC. Sensitivity in epoxide binder was comparable to PC but in the other binders it was about one order of magnitude lower.

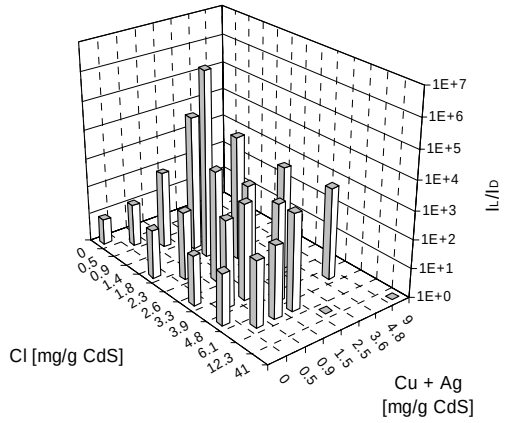

Fig. 10. Dependence of I_L/I_D ratio on the concentrations of dopants. Samples are prepared using epoxide binder.

Table 3. Comparison of polymer binders using powder E (σ = standard deviation).

Polymer	I_L/I_D	σ
PMMA	1.3×10^5	0.2×10^5
PVCA	1.7×10^5	0.2×10^5
PS	4.7×10^5	0.7×10^5
Epoxide	1.3×10^6	0.3×10^6
PC	2.4×10^6	0.5×10^6

4. Conclusions

The experimental results can be summarized as follows:

1. Dopants used for CdS activation supported the transformation from cubic to hexagonal phase. $AgNO_3$ and $CuCl_2$ at concentrations 0.24 mg Ag and 1.20 mg Cu /1g CdS or $MnCl_2$ at concentration 1.36 mg Mn/1g CdS were high enough to cause complete tranformation.
2. Incorporation of chloride into starting cadmium sulfide improved crystalline structure and the found band gap energy increased from 2.27 to 2.38 eV.
3. Reflectivities of all powders in the region of wavelengths shorter than absorption edge position were similar, about 12%. In the region around 900 nm the reflectivities depended on dopant concentrations. The highest value showed the undoped sample A; the reflectivity decreased with the growing content of acceptors (Cu, Ag). For the same acceptor dose, reflectivity decreased with growing chloride amount.
4. Epoxide binder cured at 180 °C decreased spectral reflectivity of samples which are chloride doped without the presence of Cu, Ag.
5. Doses of radiation absorbed in layers containing polymer binder increased with growing amounts of dopants, but the highest photosensitivity expressed as the ratio of photocurrent and dark current appeared at low dopant levels. Among the selected binders polycarbonate made possible to prepare the samples with the highest photosensitivity. Samples based on epoxide binder fell behind by factor lower than 2. Both polymers contain bisphenol A group in the chain. Samples based on the other selected polymers (PMMA, PVCA, PS) exhibited the photosensitivity lower by one order of magnitude.

Acknowledgement

The financial support of Ministry of Industry and Trade of the Czech Republic (grant No. FTA-TA2/018) and support from the Academy of Sciences of the Czech Republic (project Contract No. AVOZ 404 00503) are gratefully acknowledged.

References

[1] Ch. Kittel, Introduction to Solid State Physics, John Wiley & Sons, New York (1976).
[2] R. H. Bube, Photoconductivity of solids, John Wiley & Sons, New York (1960).
[3] M. Jedlička, Fotoelektrický jev (Photoelectric Effect), SNTL Press, Prague (1975).
[4] H. H. Woodbury, Physics and Chemistry of II-VI Compounds (ed. M. Aven and J. S. Prener), North-Holland publishing, Amsterdam (1967)
[5] J. Hagen, W. Schaffrath, P. Otschik, R. Fink, A. Bacher, H.-W. Schmidt, D. Haarer, Synth. Met. **89,** 215 (1997).
[6] M. Prudenziati, B. Morten, Microelectron. J. **23,** 133 (1992).
[7] S. Rothschild, J. Opt. Soc. Am. **46,** 662 (1956).
[8] S. M. Thomsen, R. H. Bube, Rev. Sci. Instrum. **26,** 664 (1955).
[9] F. H. Nicoll, B. Kazan, J. Opt. Soc. Am. **45,** 647 (1955).
[10] R. H. Bube, A. B. Dreeben, Phys. Rev. **115,** 1578 (1959).
[11] R. H. Bube, J. Appl. Phys. **31,** 2239 (1960).
[12] T. Rajh, J. Rabani, Langmuir **7,** 2054 (1991).

[13] Y. Wang, N. Herron, Chem. Phys. Lett. **200,** 71 (1992).
[14] N. C. Greenham, X. Peng, A.P. Alivisatos, Phys. Rev. B **54,** 17628 (1996).
[15] K. M. Coakley, M. D. McGehee, Chem. Mater. **16,** 4533 (2004).
[16] Ya. I. Vertsimakha, Mol. Cryst. Liquid. Cryst. **355,** 275 (2001).
[17] H. Yoneyama, M. Tokuda, S. Kuwabata, Electrochim. Acta **39,** 1315 (1994).
[18] Y. Xi, J. Zhou, H. Guo, Ch. Cai, Z. Lin, Chem. Phys. Lett. **412,** 60 (2005).
[19] D. Patidar, N. Jain, N. S. Saxena, K. Sharma, T. P. Sharma, Brasilian Journal of Physics **36**, 1210 (2006)
[20] T. Dannhauser, M. O'Neil, K. Johansson, D. Whitten, G. McLendon, J. Phys. Chem. **90,** 6074 (1986).
[21] Y. Wang, A. Suna, J. McHugh, E. Hilinski, P. Lucas, R. D. Johnson, J.Chem. Phys. **92,** 6927 (1990).
[22] P. Kubelka, F. Munck, Zeits. f. techn. Physik **12,** 593 (1931).
[23] L. Yang, B. Kruse, J. Optical Society of America A, **21,** 1933 (2004).
[24] L. A. Patil, P. A. Wani, D. P. Amalnerkar, Materials Chemistry and Physics **61,** 260 (1999).
[25] A. G. Fischer, R. J. Paff , J. Phys. Chem. Sol. **23,** 1479 (1962).
[26] W. L. Roth, Physics and Chemistry of II-VI Compounds (ed. M. Aven and J.S.Prener), North-Holland publishing, Amsterdam (1967).
[27] S. Ibuki, H. Yamashita, J. Phys. Soc. Jap. **14,** 1827 (1959).
[28] R. L. Clarke, J. Appl. Phys. **30,** 957 (1959).
[29] W. J. Moore, Physical Chemistry, Prentice Hall, Englewood Cliffs, N.Y., USA (1972).
[30] R. Pappalardo, R. E. Dietz, Phys. Rev. **123,** 1188 (1961).
[31] J. C. de Vos, Physica **20,** 690 (1954).

*Corresponding author:jiri.franc@jh-inst.cas.cz